Possibilistic Versus Belief Function Fusion for Antipersonnel Mine Detection

Nada Milisavljević and Isabelle Bloch, *Member, IEEE*

***Abstract*—Two approaches for combining humanitarian mine detection sensors are presented—one based on belief functions and the other one based on possibility theory. The approaches are described in parallel. First, different measures are extracted from the sensor data. Mass functions and possibility distributions are then derived from the measures based on prior information. After that, the combination of masses and the combination of possibility degrees are performed in two steps, on a separate sensor level and between the sensors. Combination operators are chosen to account for different characteristics of the sensors. The selection of the decision rules is discussed for both approaches. The proposed approaches are illustrated on a set of real mines and nondangerous objects, and promising results have been obtained.**

***Index Terms*—Knowledge representation, multisensor systems, possibility theory.**

I. Introduction

DUE TO a large variety of types of mines and of conditions in which mines can be found, there is no single sensor used in humanitarian mine detection that can reach the necessarily high detection rate in all possible scenarios. Therefore, an attractive way toward finding a solution is in taking the best from several complementary sensors. One of the most promising sensor combinations consists of an infrared (IR) camera, an imaging metal detector (MD), and ground-penetrating radar (GPR). In this paper, we present and compare two approaches for combining these sensors, which can be easily adapted for other sensors and their combinations. These approaches, based on belief function theory [1] and on possibility theory [2], are aimed at dealing with antipersonnel (AP) mines in a humanitarian demining context.

Most of the work done in the field of fusion of dissimilar mine detection sensors is based on statistical approaches [3]–[6]. Examples of alternative approaches are provided in [7] (fuzzy fusion of classifiers), [8] (log-likelihood ratio-test-based algorithm fusion), and [9] and [10] (neural networks). Statistical approaches lead to good results for a particular scenario; however, they often ignore or just briefly mention that several important problems have to be faced in this domain of application [5], [11], [12] once more general solutions are looked for. Namely, the data are highly variable depending on the context and conditions. In addition, the data are not numerous enough to allow for reliable statistical learning [13]. Furthermore, the data do not give precise information on the type of mine (ambiguity between several types), and it is not possible to model every object (neither mines nor objects that could be confused with them). Some fusion attempts in this domain of application treat every alarm as a mine, and not as an object that not only could be a mine but a false alarm as well [14], [15]. Last, as shown in [16], the issue of statistical correlation among the outputs of demining sensors is not always taken into account in statistical approaches and typically leads to reduced performance.

In a previous work [17], a method based on the belief function theory [1], [18], [19] has been proposed. In this paper, we compare it with an alternative approach, based on the possibility theory [2], to take advantage of the flexibility in the choice of combination operators [20], [21]. This aspect is exploited here to account for different characteristics of the sensors to be combined. In various remote-sensing applications, these fusion methods have been successfully used [22]–[27]. However, to our knowledge, in the domain of AP mine detection, there is no attempt to apply the two fusion theories in parallel and/or to compare them. In other domains, there are some works that compare the two approaches, such as [28], where the belief function theory is opposed to the qualitative possibility theory and illustrated on a fictitious example of the assessment of the value of a candidate. In contrast to that paper, we apply the quantitative possibility theory here.

According to the general scheme of fusion described in [29], the main steps of our two approaches, presented in parallel, include modeling of the available information and data (Section II), combination (Section III), and a final decision step (Section IV). Results obtained on data acquired at the Netherlands Organization for Applied Scientific Research test facilities [30] within the Dutch HOM-2000 project, containing a set of real mines and nondangerous objects, are shown and compared in Section V.

II. Information Modeling

From the data gathered by the sensors, a number of measures are extracted, as in [17]. These measures concern the following:

- area and the shape (elongation and ellipse fitting) of the object observed using the IR sensor;

Manuscript received September 24, 2007; revised October 23, 2007. This work was supported in part by the Belgian Ministry of Defense within the BElgian contribution to Mine Action Technologies (BEMAT project).

N. Milisavljević is with Signal and Image Centre, Royal Military Academy, 1000 Brussels, Belgium (e-mail: nada@elec.rma.ac.be).

I. Bloch is with the Département Traitement du Signal et des Images, Ecole Nationale Supérieure des Télécommunications, Centre National de la Recherche Scientifique Unité Mixte de Recherche 5141, Laboratoire Traitement et Communication de l'Information, 75634 Paris, France (e-mail: isabelle.bloch@enst.fr).

Color versions of one or more of the figures in this paper are available online at http://ieeexplore.ieee.org.

Digital Object Identifier 10.1109/TGRS.2008.916210

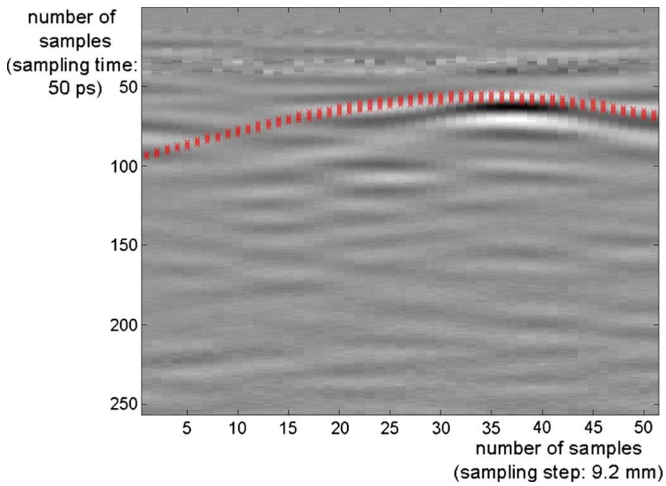

Fig. 1. Example of the GPR data (B-scan after background removal) and the extracted hyperbola.

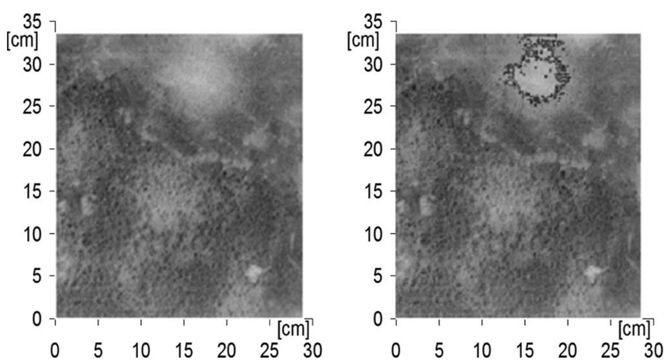

Fig. 2. Example of (left) the raw IR data together with (right) the extracted shape.

- size of the metallic area in the MD data;
- propagation velocity (thus, the type of material), the burial depth of the object observed using the GPR, and the ratio between the object size and its scattering function.

As an illustration, Fig. 1 contains a preprocessed B-scan (2-D image representing a vertical slice in the ground, along the scanning direction) of the GPR data. Due to poor directivity of the transmitting and receiving antennas of the GPR, an object leaves a hyperbolic signature in a B-scan. If this hyperbola is well detected, as in Fig. 1, the three GPR measures can be directly related to the extracted hyperbola parameters [31]. Mass functions and possibility distributions are then derived from the measures based on prior information, such as the usual size of mines or the typical burial depth.

An example of the IR data is given in Fig. 2 (left), taken at the optimum time of the day for the IR measurements (periods of higher temperature contrasts between potential objects and the soil) [32]. After some preprocessing, extraction of a region having a high contrast with the surroundings is performed, as shown in Fig. 2 (right). In brief, the region selection method, introduced in [33], consists of estimating a background from

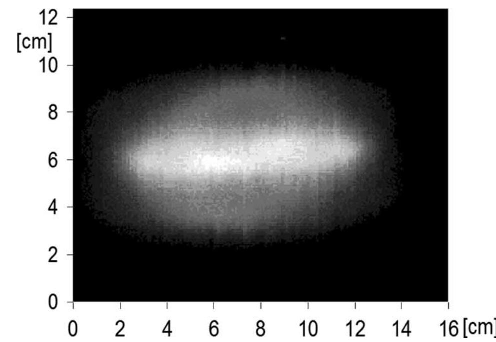

Fig. 3. Example of the raw MD data.

a preset number of the bordering pixels around an image and preserving the pixels that significantly differ from the estimated background.

Fig. 3 illustrates the MD data gathered over an x-like metallic shape. The raw image is blurred mainly due to a large footprint of the MD coil with respect to the size of metallic objects such as mines. In reality, the MD images are sometimes saturated, so it is not possible to recover the true shape using classical restoration techniques [34], and the raw image is analyzed further [33].

In the following, we model the information provided by these measures in terms of possibility distributions as well as mass functions. Note that we have two spaces for each function—the set of hypotheses, which is the same for each function, and the feature space, which depends on the measurements from which the function is derived. Each function for one hypothesis is, therefore, not a value, but a function over the feature space (a function of the depth value, of the shape measure, etc.). The specific shape of the functions and their parameters are derived from the knowledge, indicating their general behavior.

A. IR Measures

Elongation and ellipse fitting measures provide information mainly on shape regularity [17]. The possibility degrees of being a regular-shaped mine (MR), derived from these two measures, are represented by $\pi_{1I}(MR)$ and $\pi_{2I}(MR)$. Similarly, $\pi_{1I}(MI)$ and $\pi_{2I}(MI)$ denote the possibility degrees of being an irregular-shaped mine (MI). Then, the possibility degrees of being a regular-shaped nondangerous (i.e., friendly) object (FR) and an irregularly shaped friendly object (FI) are defined too and are denoted by $\pi_{1I}(FR)$ and $\pi_{1I}(FI)$ for elongation measure, and by $\pi_{2I}(FR)$ and $\pi_{2I}(FI)$ for ellipse fitting measure, respectively.

In terms of belief functions, the frame of discernment (full set) is $\Theta = \{MR, MI, FR, FI\}$. As elongation and ellipse fitting aim at distinguishing regular and irregular shapes, masses assigned by these two measures, m_{1I} and m_{2I}, are split between $MR \cup FR$, $MI \cup FI$, and the full set.

Regarding elongation, we calculate r_1 as the ratio between the minimum and maximum distances of bordering pixels from the center of gravity (we work on thresholded images), and r_2 as the ratio of minor and major axes obtained from second-moment calculation [17], [35]. Using these two ratios, the following possibility degrees are derived:

$$\pi_{1I}(MR) = \pi_{1I}(FR) = \min(r_1, r_2) \tag{1}$$

$$\pi_{1I}(MI) = \pi_{1I}(FI) = 1 - \pi_{1I}(MR). \tag{2}$$

In the framework of belief functions, for this measure, masses are defined as follows:

$$m_{1I}(MR \cup FR) = \min(r_1, r_2) \tag{3}$$

$$m_{1I}(MI \cup FI) = |r_1 - r_2| \tag{4}$$

and the full set takes the rest, i.e.,

$$m_{1I}(\Theta) = 1 - \max(r_1, r_2). \tag{5}$$

In case of ellipse fitting, let A_{oe} be the part of an object area that belongs to the fitted ellipse as well, A_o be the object area, and A_e be the ellipse area. Then, we define

$$\pi_{2I}(MR) = \pi_{2I}(FR) = \max\left(0, \min\left\{\frac{A_{oe}-5}{A_o}, \frac{A_{oe}-5}{A_e}\right\}\right) \tag{6}$$

$$\pi_{2I}(MI) = \pi_{2I}(FI) = 1 - \pi_{2I}(MR). \tag{7}$$

Masses for this measure are the following ones [17]:

$$m_{2I}(MR \cup FR) = \max\left(0, \min\left\{\frac{A_{oe}-5}{A_o}, \frac{A_{oe}-5}{A_e}\right\}\right) \tag{8}$$

$$m_{2I}(MI \cup FI) = \max\left\{\frac{A_e - A_{oe}}{A_e}, \frac{A_o - A_{oe}}{A_o}\right\} \tag{9}$$

$$m_{2I}(\Theta) = 1 - m_{2I}(MR \cup FR) - m_{2I}(MI \cup FI). \tag{10}$$

The subtraction of five pixels is introduced to include the limit case of an ellipse (minimum of five points needed to define it), where we cannot judge about the shape at all, so ignorance should be maximum.

Note that in cases where reliable information exists that all mines have a regular shape, the possibility degrees of MR can be reassigned to mines of any shape ($M = MR \cup MI$), whereas the possibility degrees of MI can be reassigned to friendly objects of any shape ($F = FR \cup FI$). Similarly, masses given to $MR \cup FR$ can be reassigned to M, whereas masses given to $MI \cup FI$ can be reassigned to F.

The area directly provides a degree $\pi_{3I}(M)$ of being a mine. Namely, since the range of possible AP mine sizes is approximately known, the degree of possibility of being a mine is derived as a function of the measured size

$$\pi_{3I}(M) = \frac{a_I}{a_I + 0.1 \cdot a_1} \cdot \exp \frac{-\left[a_I - 0.5 \cdot (a_1 + a_2)\right]^2}{0.5 \cdot (a_2 - a_1)^2} \tag{11}$$

where a_I is the actual object area on the IR image, whereas the approximate range of expectable mine areas is between a_1 and a_2 (for AP mines, it is reasonable to set $a_1 = 15$ cm^2 and $a_2 = 225$ cm^2 [17], [36]). On the contrary, friendly objects can be of any size, so the measured size is uninformative about the possibility of being a friendly object. Hence, the possibility degree is set to 1 whatever the value of the size, i.e.,

$$\pi_{3I}(F) = 1. \tag{12}$$

As anything could have the same area/size as a mine, while outside the range of the expected size of mines, it is far more probable that the object is friendly; area/size mass assignment is given by the following two equations [17]:

$$m_{3I}(\Theta) = \frac{a_I}{a_I + 0.1 \cdot a_1} \cdot \exp \frac{-\left[a_I - 0.5 \cdot (a_1 + a_2)\right]^2}{0.5 \cdot (a_2 - a_1)^2} \tag{13}$$

$$m_{3I}(FR \cup FI) = 1 - m_{3I}(\Theta). \tag{14}$$

B. MD Measures

If the point-spread function (impulse response) of the MD is known, if the gathered data are not saturated, and if the scanning step in both directions is small enough, it is possible to extract the object shape and area as seen by the MD, as well as the burial depth [34], [37], [38]. In that case, the latter measure can be modeled as the GPR burial depth measure (see Section II-C), whereas the shape and area measures can be modeled as in Section II-A (the IR case), but the results should be treated with caution as the meanings of the shape and of the area are related to the amount of metal in the object (metallic pieces in low-metal-content mines may have complicated shapes, and they are not in contact with the host soil) [38], [39]. In reality, if the range of existing metal contents expected in the field is very wide, depending on the type of the MD used, it can be difficult to adjust the sensitivity, so that all the low-metal-content mines are detected without causing the data saturation for high-metal-content objects [34]. Furthermore, if the minefield is large, to speed up the scanning time, the data-gathering resolution in the cross-scanning direction can be very poor, as it is the case with the data used in this paper. Thus, the MD information used here consists of only one measure, which is the width of the region in the scanning direction w (in centimeters; as shown in [17], other measures can be easily added). As friendly objects can contain metal of any size, we define

$$\pi_{\mathrm{MD}}(F) = 1. \tag{15}$$

On the contrary, if there is some knowledge on the expected sizes of metal in mines (for many AP mines, this range is between 5 and 15 cm), we can assign possibilities to mines as, e.g.,

$$\pi_{\mathrm{MD}}(M) = \frac{w}{20} \cdot [1 - \exp(-0.2 \cdot w)] \cdot \exp\left(1 - \frac{w}{20}\right). \tag{16}$$

The corresponding mass functions are [17]

$$m_{\mathrm{MD}}(\Theta) = \frac{w}{20} \cdot [1 - \exp(-0.2 \cdot w)] \cdot \exp\left(1 - \frac{w}{20}\right) \tag{17}$$

$$m_{\mathrm{MD}}(FR \cup FI) = 1 - m_{\mathrm{MD}}(\Theta). \tag{18}$$

C. GPR Measures

All the three GPR measures provide information about mines [31].

In case of burial depth information D, friendly objects can be found at any depth, whereas it is known that there is some maximum depth up to which AP mines can be expected. They can rarely be found buried below 25 cm $(D_{\max})$, often much shallower, the depth being limited mainly by their activation principles. However, due to soil perturbations, erosions, etc., mines can, by time, go deeper or shallower than the depth at which they were initially buried. Thus, for this GPR measure, the possibility distributions for mines, i.e., $\pi_{1G}(M)$, and friendly objects, i.e., $\pi_{1G}(F)$, can be modeled as follows:

$$\pi_{1G}(M) = \frac{1}{\cosh(D/D_{\max})^2} \tag{19}$$

$$\pi_{1G}(F) = 1. \tag{20}$$

The masses for this measure are [31] given by

$$m_{1G}(\Theta) = \frac{1}{\cosh(D/D_{\max})^2} \tag{21}$$

$$m_{1G}(FR \cup FI) = 1 - m_{1G}(\Theta). \tag{22}$$

Another GPR measure exploited here is the ratio d/k (corresponding to the opening of the hyperbola [31]) between the object size seen in the scanning direction d and its scattering function k directly related to the object shape [40]. Again, friendly objects can have any value of this measure, whereas for mines, there is a range of values that mines can have, and outside that range, the object is quite certainly not a mine, i.e.,

$$\pi_{2G}(M) = \exp\left(-\frac{[(d/k) - m_d]^2}{2 \cdot p^2}\right) \tag{23}$$

$$\pi_{2G}(F) = 1 \tag{24}$$

where m_d is the d/k value at which the possibility distribution reaches its maximum value (here, $m_d = 700$, chosen based on prior information [40]), and p is the width of the exponential function (here, $p = 400$).

Similarly, the mass assignments for this measure are [31]

$$m_{2G}(\Theta) = \exp\left(-\frac{[(d/k) - m_d]^2}{2 \cdot p^2}\right) \tag{25}$$

$$m_{2G}(FR \cup FI) = 1 - m_{2G}(\Theta). \tag{26}$$

Last, propagation velocity v can provide information about object identity. Here, we extract depth information on a different way than in the case of the burial depth measure [31], and we preserve the sign of the extracted depth. This information indicates whether a potential object is above the surface. If that is the case, the extracted propagation velocity should be close to $c = 3 \times 10^8$ m/s, the propagation velocity in vacuum. Otherwise, if the sign indicates that the object is below the soil surface, the value of v should be around the values for the corresponding medium, e.g., from 5.5×10^7 to 1.73×10^8 m/s [40] in the case of sand, i.e.,

$$\pi_{3G}(M) = \exp\left(-\frac{(v - v_t)^2}{2 \cdot h^2}\right) \tag{27}$$

where v_t is the value of velocity that is the most typical for the medium (here, for sand, it is $0.5 \times (5.5 \times 10^7 + 1.73 \times 10^8) = 1.14 \times 10^8$ m/s, and for air, it is equal to c), and h is the width of the exponential function (here, $h = 6 \times 10^7$ m/s). If the extracted velocity value significantly differs from the expected values for that medium, it can be expected that there is no object indeed, so, again, friendly objects can have any value of the velocity, i.e.,

$$\pi_{3G}(F) = 1. \tag{28}$$

The corresponding mass functions are [31]

$$m_{3G}(\Theta) = \exp\left(-\frac{(v - v_{\max})^2}{2 \cdot h^2}\right) \tag{29}$$

$$m_{3G}(FR \cup FI) = 1 - m_{3G}(\Theta). \tag{30}$$

D. Comparison of Both Models

Let us briefly comment on the similarities and the differences in both models. Although the semantics is different, similar information can be modeled. The idea behind this paper is to design the possibility and mass functions as similarly as possible to concentrate on the comparison at the combination step.

The main difference relies in the modeling of ambiguity. The semantics of possibility leads to model ambiguity between two hypotheses with the same degrees of possibilities for these two hypotheses. This is, for example, the case in (1) and (6). On the contrary, the reasoning on the power set of hypotheses in the belief function theory leads to assigning a mass to the union of these two hypotheses, and examples are (3) and (8).

Another distinction concerns the ignorance. Although it is explicitly modeled in the belief function theory through a mass on the whole set (to guarantee the normalization of the mass function over the power set), it is only implicitly expressed in the possibilistic model through the absence of a normalization constraint.

III. Combination

The combination of possibility degrees, as well as of masses, is performed in two steps. The first one applies to all measures derived from one sensor. The second one combines results obtained in the first step for all three sensors.

A. Combination of Possibility Degrees

Here, only the combination rules related to mines are considered. The issue of combination rules for friendly objects is discussed in Section IV-A.

Let us first detail the first step for each sensor. For the IR, since mines can be regular or irregular, the information about regularity on the level of each shape measure is combined using a disjunctive operator (here, the max), i.e.,

$$\pi_{1IM} = \max\left(\pi_{1I}(MR), \pi_{1I}(MI)\right) \tag{31}$$
$$\pi_{2IM} = \max\left(\pi_{2I}(MR), \pi_{2I}(MI)\right). \tag{32}$$

The choice of the maximum (smallest disjunction and idempotent operator) as a t-conorm is related to the fact that the measures cannot be considered as completely independent from each other. Therefore, there is no reason to reinforce the measures by using a larger t-conorm, and the idempotent one is preferable in such situations. These two shape constraints should be both satisfied to have a high degree of possibility of being a mine [17]. Therefore, they are combined in a conjunctive way (here, using a product). Last, the object is possibly a mine if it has a size in the expected range or, if it is not in the expected range, satisfies the shape constraint. Hence, the final combination for the IR is

$$\pi_I(M) = \pi_{3I}(M) + [1 - \pi_{3I}(M)] \cdot \pi_{1IM} \cdot \pi_{2IM}. \tag{33}$$

The conjunction in the second term guarantees that $\pi_I(M)$ is in [0, 1].

In case of the GPR, it is possible to have a mine if the object is at shallow depths and its dimensions resemble a mine, and the extracted propagation velocity is appropriate for the medium. Thus, the combination of the obtained possibilities for mines is performed using a t-norm, expressing the conjunction of all criteria. Here, the product t-norm is used, i.e.,

$$\pi_G(M) = \pi_{1G}(M) \cdot \pi_{2G}(M) \cdot \pi_{3G}(M). \tag{34}$$

For the MD, as there is just one measure used, there is no first combination step, and the possibility degrees obtained using (7) and (8) are directly used.

In case of possibilities, the second combination step is performed using the following algebraic sum:

$$\begin{aligned}\pi(M) = &\pi_I(M) + \pi_{\mathrm{MD}}(M) + \pi_G(M) - \pi_I(M) \cdot \pi_{\mathrm{MD}}(M)\\ &- \pi_I(M) \cdot \pi_G(M) - \pi_{\mathrm{MD}}(M) \cdot \pi_G(M)\\ &+ \pi_I(M) \cdot \pi_{\mathrm{MD}}(M) \cdot \pi_G(M)\end{aligned} \tag{35}$$

leading to a strong disjunction [20], [41] since the final possibility should be high if at least one sensor provides a high possibility. This operator is also chosen based on the fact that it is better to assign a friendly object to the mine class than to miss a mine.

B. Combination of Masses

For the IR and the GPR, masses assigned by the measures of each of the two sensors are combined by Dempster's rule in an unnormalized form [1], [19], i.e.,

$$m_{ij}(S) = \sum_{\substack{k,l \\ A_k \cap B_l = S}} m_i(A_k) \cdot m_j(B_l) \tag{36}$$

where S is any subset of the full set, whereas m_i and m_j are masses assigned by measures i and j, and their focal elements are $A_1, A_2, \ldots, A_p$ and $B_1, B_2, \ldots, B_q$, respectively. Dempster's rule is commutative and associative, which means that it can be repeatedly applied until all measures are combined, and that the result does not depend on the order used in the combination. A general idea for using the unnormalized form of this rule instead of the more usual normalized form is to preserve conflict [17], [42], that is, mass assigned to the empty set, i.e.,

$$m_{ij}(\varnothing) = \sum_{\substack{k,l \\ A_k \cap B_l = \varnothing}} m_i(A_k) \cdot m_j(B_l). \tag{37}$$

Here, a high degree of conflict would indicate that either there are several objects, and the sensors, as detectors of different physical phenomena, do not provide information on the same object, or some sources of information are not completely reliable. Our main interest is in the possibility that sensors do not refer to the same object, as the unreliability can be modeled and resolved through discounting factors [17].

After combining masses per sensor, the fusion of sensors is performed using Dempster's rule in the unnormalized form [see (36)]. If the mass of the empty set after the combination of sensors is high, they should be clustered, as they do not sense the same object.

In this framework, two other functions are usually derived from the mass functions, i.e., beliefs Bel and plausibilities Pl [1], that are defined in the following way for any subset B:

$$Bel(B) = \sum_{S \subseteq B, S \neq \varnothing} m(S) \tag{38}$$
$$Pl(B) = \sum_{S \cap B \neq \varnothing} m(S). \tag{39}$$

C. Comparison of the Combination Equations

For the IR, from (1)–(14), it is evident that

$$\pi_{1I}(MR) = m_{1I}(MR \cup FR) \tag{40}$$
$$\pi_{1I}(MI) = m_{1I}(MI \cup FI) \tag{41}$$
$$\pi_{2I}(MR) = m_{2I}(MR \cup FR) \tag{42}$$
$$\pi_{2I}(MI) = m_{2I}(MI \cup FI) \tag{43}$$
$$\pi_{3I}(M) = m_{3I}(\Theta) \tag{44}$$

so (33) can be rewritten as

$$\pi_I(M) = m_{3I}(\Theta) + [1 - m_{3I}(\Theta)] \cdot m_{1IM} \cdot m_{2IM} \tag{45}$$

with

$$m_{1IM} = \max\left(m_{1I}(MR \cup FR), m_{1I}(MI \cup FI)\right) \tag{46}$$
$$m_{2IM} = \max\left(m_{2I}(MR \cup FR), m_{2I}(MI \cup FI)\right). \tag{47}$$

For this sensor, the combination of masses using (36) and the calculation of plausibilities based on (39) lead to

$$Pl_I(M) = m_{3I}(\Theta) \cdot [m_{12I}(\Theta) + m_{12I}(MR \cup FR) + m_{12I}(MI \cup FI)] \quad (48)$$

where m_{12I} are the masses resulting from the combination of m_{1I} and m_{2I} (elongation and ellipticity). As the focal elements of these two mass functions are $MR \cup FR$, $MI \cup FI$, and the full set, the combination also results in the empty set mass (37), i.e.,

$$m_{12I}(\varnothing) = 1 - [m_{12I}(\Theta) + m_{12I}(MR \cup FR) + m_{12I}(MI \cup FI)] \geq 0. \quad (49)$$

From (48) and (49), we can write

$$Pl_I(M) \leq m_{3I}(\Theta) \quad (50)$$

which means that based on (45)

$$Pl_I(M) \leq \pi_I(M). \quad (51)$$

This is in accordance with the least commitment principle used in the possibilistic model, as usually done in this framework.

As far as the MD is concerned, there is no difference since it provides only one measure.

In case of the GPR, based on the comparison of (19) and (21), (23) and (25), as well as (27) and (29), we can conclude that

$$\pi_{1G}(M) = m_{1G}(\Theta) \quad (52)$$

$$\pi_{2G}(M) = m_{2G}(\Theta) \quad (53)$$

$$\pi_{3G}(M) = m_{3G}(\Theta). \quad (54)$$

Hence, we can rewrite (34) as

$$\pi_G(M) = m_{1G}(\Theta) \cdot m_{2G}(\Theta) \cdot m_{3G}(\Theta). \quad (55)$$

Furthermore, the application of Dempster's rule [see (36)] to the mass assignments of the three GPR measures results in the fused mass of the full set for this sensor, i.e.,

$$m_G(\Theta) = m_{1G}(\Theta) \cdot m_{2G}(\Theta) \cdot m_{3G}(\Theta) \quad (56)$$

which leads to

$$\pi_G(M) = m_G(\Theta). \quad (57)$$

This means that the ignorance is modeled as a mass on Θ in the belief function framework, whereas it privileges the class that should not be missed (M) in the possibilistic framework (i.e., the ignorance will lead to safely decide in favor of mines).

D. About Combination Operators in Possibilistic Fusion

Each combination rule selected in the possibilistic method (Section III-A) reflects logical reasoning. Different operators for conjunctive and disjunctive combinations exist [21], [29], [41]. To test the influence of the choice of the operator, we select two frequently used conjunctive operators (minimum and product) and two disjunctive operators (maximum and algebraic sum). For each combination, we alter the two operators from the same family.

For the IR, as explained in Section III-A, (33) is based on the logic that each shape constraint should provide maximum information regarding the mine (therefore, disjunctive combination); the two shape constraints should be combined in a conjunctive way and then combined with the size in a disjunctive way. There is no reason to apply different operators to each of the two shape constraints; thus, we alter three combination operators—a disjunctive operator for each of the shape constraints (let us call it operator f), a conjunctive operator for combining the two of them (operator g), and a disjunctive operator for combining their combination with the third size measure (operator h). Based on our selection of two conjunctive and two disjunctive operators, f can be the maximum or the algebraic sum, g can be the product or the minimum, and h can be the maximum or the algebraic sum. Taking into account the fact that the product is always less than or equal to the minimum, whereas the maximum is always less than or equal to the algebraic sum, the highest values of the possibility degrees for mines in these conditions would be obtained if f is the algebraic sum, g is the minimum, and h is the algebraic sum, i.e.,

$$\pi_{I\max}(M) = \pi_{3I}(M) + [1 - \pi_{3I}(M)] \cdot (\pi_{1IN}, \pi_{2IN}) \quad (58)$$

where

$$\pi_{1IN} = \pi_{1I}(MR) + \pi_{1I}(MI) - \pi_{1I}(MR) \cdot \pi_{1I}(MI) \quad (59)$$

$$\pi_{2IN} = \pi_{2I}(MR) + \pi_{2I}(MI) - \pi_{2I}(MR) \cdot \pi_{2I}(MI). \quad (60)$$

Similarly, the lowest values of the possibility degrees for mines would be obtained if f is the maximum, g is the product, and h is the maximum, i.e.,

$$\pi_{I\min}(M) = \max\left(\pi_{3I}(M), (\pi_{1IM} \cdot \pi_{2IM})\right). \quad (61)$$

In case of the GPR, (34) is obtained based on the logic that the three measures should be combined in the conjunctive way. Again, there is no reason to use different types of similar operators between the sensors. Since we alter two operators from the same group, there is only one alternative to be tested, i.e.,

$$\pi_{G1}(M) = \min\left(\pi_{1G}(M), \pi_{2G}(M), \pi_{3G}(M)\right). \quad (62)$$

As the product is always less than or equal to the minimum, it is sure that $\pi_G(M) \leq \pi_{G1}(M)$.

Similarly, for the second combination step, where the disjunctive combination of the three sensors should be used, the only alternative for (35) in our tests is

$$\pi_1(M) = \max\left(\pi_I(M), \pi_{MD}(M), \pi_G(M)\right). \quad (63)$$

Since the maximum is always less than or equal to the algebraic sum, it is certain that $\pi(M) \geq \pi_1(M)$.

Results on real data of these alternative equations are shown and discussed in Section V-B.

IV. Decision

As the final decision about the identity of the object should be left to the deminer not only because his life is in danger but also because of his experience, the fusion output is a suggested decision together with confidence degrees.

A. Possibilistic Fusion

In case of possibilities, the final decision is simply obtained by thresholding the fusion result for M and providing the corresponding possibility degree as the confidence degree. Since almost all possibility degrees obtained at the fusion output are either very low or very high, the selected regions having very low values of $\pi(M)$ (below 0.1) are classified as F, and the ones with very high values (above 0.7) are classified as M. There are only a few regions at which the resulting possibility degree for M has an intermediary value. In these cases, as mines must not be missed, the decision is M. In the following, this decision approach is referred to as *dec*1.

An alternative (*dec*2) for the final decision making is to derive the combination rule for F as well, compare the final values for M and F, and derive an adequate decision rule. Due to the operation principles of the GPR and the MD, the measures of these two sensors can only give information where mines are possibly not; however, they cannot say where friendly objects can or cannot be. For example, it is equally possible, in reality, to have friendly objects (a placed friendly object or a clutter-caused alarm) at any depth or of any size. As they are noninformative with respect to friendly objects, it is not useful to combine their possibility degrees for F. Thus, for deriving the final combination rule for F, i.e., $\pi(F)$, we can rely only on the IR, i.e.,

$$\pi(F) = \pi_1(F). \tag{64}$$

In case of the IR, since friendly objects can be regular or irregular, we apply a disjunctive operator (the maximum) for each of the shape constraints. To be cautious when deciding F, we combine the two shape constraints and the size measure using a conjunctive operator, which means that the possibility degree for F should be high only if all three measures should favor F. Taking into account (12), this reasoning results in

$$\pi(F) = \max\left(\pi_{1I}(F_R), \pi_{1I}(F_I)\right) \cdot \max\left(\pi_{2I}(F_R), \pi_{2I}(F_I)\right). \tag{65}$$

Thus, in this alternative way to derive decisions, in regions where the IR gives an alarm, the decision rule chooses M or F depending on which one of the two has a higher possibility value, given by (35) and (65), respectively. In other regions, at which the IR does not give an alarm, although at least one of the two other sensors gives an alarm, the decision is based on the fusion result for M, as in *dec*1.

B. Belief Function Fusion

In case of belief functions, as shown in [17], usual decision rules based on beliefs, plausibilities [1], and pignistic probabilities [43] do not give useful results because there are no focal elements containing mines alone [42]. The underlying reason is that the sensors used in humanitarian demining are not mine detectors but anomaly detectors, so whenever they detect something that could be a mine, it could be anything else as well. As a consequence, these usual decision rules would always favor friendly objects.

In such a sensitive application as humanitarian demining, no mistakes are allowed, so in case of any ambiguity, much more importance should be given to mines. Because of that, in [17], guesses $G(A)$ are defined, where $A \in \{M, F, \varnothing\}$, i.e.,

$$G(M) = \sum_{M \cap B \neq \varnothing} m(B) \tag{66}$$

$$G(F) = \sum_{B \subseteq F, B \neq \varnothing} m(B) \tag{67}$$

$$G(\varnothing) = m(\varnothing). \tag{68}$$

In other words, the guess value of a mine is the sum of masses of all the focal elements containing mines, regardless of their shape, and the guess of a friendly object is the sum of masses of all the focal elements containing nothing else but friendly objects of any shape, which means that the guesses are a cautious way to estimate confidence degrees.

As the output of the belief function fusion module, the three possible outputs (M, F, conflict) are provided together with the guesses for each of the sensors and for their combination.

Note that for the GPR, the focal elements are only $F(FR \cup FI)$ and Θ [31]; therefore, guesses for this sensor simply become

$$G_G(M) = m_G(\Theta) \tag{69}$$

$$G_G(F) = m_G(F). \tag{70}$$

From (57) and (69), we conclude that for the GPR, the possibility degree of a mine is equal to the guess of a mine, i.e.,

$$\pi_G(M) = G_G(M). \tag{71}$$

Furthermore, (39) and (66) show that the guess of a mine is equal to its plausibility, whereas (38) and (67) show that the guess of a friendly object is equal to its belief (which, again, reflects the fact that we should be cautious in deciding that the object is not a mine). This means that the relation given by (51) shows, actually, that for the IR

$$G_I(M) \leq \pi_I(M). \tag{72}$$

V. Results

A. Originally Selected Possibilistic Combination Rules

The proposed approach has been applied to a set of known objects, buried in sand, leading to 36 alarmed regions in total—21 mines (M), 7 placed false alarms (PF, friendly objects), and 8 false alarms caused by clutter (FN, with no object). All of the mines are small AP mines, most have little metal, and some have no metal at all. To be as close as possible to reality, the data of the three sensors were collected in same conditions (same place and time).

TABLE I
CORRECT CLASSIFICATION RESULTS, POSSIBILISTIC FUSION. M = MINES; PF = PLACED FALSE ALARMS; FN = FALSE ALARMS WITH NO OBJECT

Classified correctly, possibility theory	Sensors			Fusion	
	IR	*MD*	*GPR*	*dec1*	*dec2*
M (total: 21)	18 (18)	9 (9)	13 (13)	21 (21)	21 (21)
PF (total: 7)	0 (4)	0 (4)	2 (6)	1 (7)	2 (7)
FN (total: 8)	0 (1)	0 (0)	6 (7)	6 (8)	6 (8)

TABLE II
CORRECT CLASSIFICATION RESULTS, BELIEF FUNCTIONS. M = MINES; PF = PLACED FALSE ALARMS; FN = FALSE ALARMS WITH NO OBJECT

Classified correctly, belief functions	Sensors			*Fusion*
	IR	*MD*	*GPR*	
M (total: 21)	10 (18)	9 (9)	13 (13)	19 (21)
PF (total: 7)	3 (4)	0 (4)	1 (6)	2 (7)
FN (total: 8)	0 (1)	0 (0)	6 (7)	6 (8)

The results of the possibilistic fusion are very promising since all mines are correctly classified with the proposed approach, as can be seen in Table I. The numbers given in the parenthesis indicate the number of regions selected in the preprocessing step for further analysis, i.e., measure extraction and classification. Regarding the combination operators, the results given in this table are based on the combination proposed in Section III-A, i.e., (33)–(35). The second fusion step is important since a decision taken after the first step provides only 18 mines for the IR, 9 for the MD, and 13 for the GPR. This illustrates the interest of combining heterogeneous sensors.

The two decision rules, i.e., *dec*1 and *dec*2, give the same results for mines and friendly objects caused by clutter. In case of placed false alarms, two are correctly classified in case of *dec*2, which is a slight improvement with respect to *dec*1 and the same result as for the belief function fusion, shown in Table II (however, in practice, it would mean less time spent and less human efforts wasted on digging false alarms from the ground). It is not surprising that the placed false alarms are not so well detected by any of the methods since our model is designed to favor the detection of mines. This is also the type of results expected from deminers.

Regarding correct classification of mines, the results of the possibilistic fusion (all 21 mines detected; see Table I) are slightly better than those obtained using the belief function method (19 of 21 mines detected; see Table II). This is due to the increased flexibility at the combination level. False alarms with no objects are correctly identified by the belief function method (six out of eight), and it is the same result as for the two possibilistic decision rules. This result shows that the power of our methods is in decreasing the number of clutter-caused false alarms without decreasing the result of mine detection, thanks to knowledge inclusion.

All results have been obtained with the models proposed in Section II, with the same parameters. It should be noted that although the general shapes of the possibility distributions are important and have been designed based on prior knowledge, they do not need to be estimated very precisely, and the results are robust to small changes in these functions. What is important is that the functions are not crisp (no thresholding approach is used), and that the rank is preserved (e.g., an object with a measure value outside of the usual range should have a lower possibility degree than an object with a typical measure value). Two main reasons explain the experienced robustness: 1) these possibility distributions are used to model imprecise information, so they do not have to be precise themselves; and 2) each of them is combined in the fusion process (Section III) with other pieces of information, which diminishes the importance and the influence of each of them.

Differences between the results of Tables I and II can be formally explained as discussed in Section III-C. For the GPR, (71) explains why the results are the same for the two fusion approaches. In case of the IR, (72) indicates that the possibilistic approach would favor mines more than the belief function approach, which is indeed the case here.

In terms of the probability of detection P_d and the false alarm rate P_f, we can conclude the following:

— for possibilistic fusion, in case of $dec1$, $P_d = 100\%$ and $P_f = 53.3\%$, whereas in case of $dec2$, $P_d = 100\%$ and $P_f = 46.7\%$ (Table I);

— for belief function fusion, $P_d = 90.5\%$ and $P_f = 46.7\%$ (Table II).

However, these values have to be cautiously considered, given the low number of examples we have.

B. Alternative Possibilistic Combination Rules

In case of the IR, tests performed using different combinations of operators f, g, and h show that, as predicted, the highest possibility degrees for mines are obtained by $\pi_{I\max}(M)$. Thus, without knowing the ground truth, this combination of operators would be the safest choice to be sure not to miss any mine (it might increase the number of false alarms, but the involved risks are certainly not the same). As expected, the lowest possibility degrees of mines are obtained in case of $\pi_{I\min}(M)$. Therefore, ignoring the ground truth, this type of combination would be the least safe choice from the point of view of humanitarian mine detection.

For the GPR, results prove the theory, i.e., $\pi_G(M) \leq \pi_{G1}(M)$, so $\pi_{G1}(M)$ would be a safer choice than $\pi_G(M)$.

Similarly, at the second combination step, using the original IR and GPR combination rules given by (33) and (34), the results prove that $\pi(M) \geq \pi_1(M)$, which means that combination (35) is a safer choice.

Therefore, without knowing the ground truth and based purely on the obtained possibilities, if we want to obtain the highest possibilities for M, our choice would be the following: $\pi_{I\max}(M)$ for the IR, $\pi_{G1}(M)$ for the GPR, and combination rule (35) for the second combination step (where $\pi_I(M)$ is replaced by $\pi_{I\max}(M)$, whereas $\pi_{G1}(M)$ is used instead of $\pi_G(M)$). In Table III, these results are referred to as $S1$; the

TABLE III
SAFEST ($s1$) VERSUS THE LEAST SAFE ($s2$) POSSIBILISTIC COMBINATIONS. M = MINES; PF = PLACED FALSE ALARMS; FN = FALSE ALARMS WITH NO OBJECT

Classified correctly	Sensors				Fusion			
	IR		*GPR*		*dec1*		*dec2*	
	S1	*S2*	*S1*	*S2*	*S1*	*S2*	*S1*	*S2*
M	18	15	13	13	21	21	21	21
PF	0	0	2	2	1	1	1	2
FN	0	0	6	6	6	6	6	6

MD results are skipped since they are the same as in Table I, as well as the number of alarmed regions and the total number of objects per type.

However, to illustrate what the consequences of the least safe choice would be, we test also the following ($S2$ in Table III): $\pi_{I\min}(M)$ for the IR, $\pi_G(M)$ for GPR, and (63) for the second combination step (where $\pi_I(M)$ is replaced by $\pi_{I\min}(M)$). Note that the results for the GPR in the $S2$ case are the same as the ones in Table I. In this illustration, for the IR, the GPR, and *dec*1 in the least safe case ($S2$), we use a threshold of 0.5 on the possibility degrees for mines (if it is above that threshold, it is M, and if it is below the threshold, it is F). The choice of this threshold is important for the IR in case $S2$, as the possibility degrees for some of the mines decrease to this level (three of them, having possibility degrees of 0.45, 0.46, and 0.46, are, thus, wrongly classified). In case of the GPR, $S1$ and $S2$ have a strong gap in the values, which means that the possibility degrees are either very high or very low, so the choice of the threshold would not change the results. For the second combination step, the possibility degrees are also very well distinguished, so the choice of the threshold is not critical. The only exceptions are one mine and one placed false alarm in case of $S2$, both reaching the possibility degree of 0.55. Note that the maximization of the safety, by making sure that the possibility degrees for mines are the highest possible ($S1$), results in the decreased classification performance for placed false alarms, and, as a consequence, the difference between *dec*1 and *dec*2, shown in Section V-A, has disappeared. This difference exists for $S2$ since the possibility results in the degrees for mines are the lowest in this case; however, another danger arises here, as these values in a few regions fall on the level of possibility degrees for friendly objects.

The analysis performed here demonstrates the robustness of the choice of the operator (within a class corresponding to the type of reasoning we want to achieve). The results in Table III illustrate this robustness very clearly: all mines are detected in the second step for all fusion schemes.

In the tests for *dec*2 given in Table III, the possibility degrees are the same as in Section V-A, calculated from (65). To analyze whether there is even a worse case than $S2$ in Table III, we test this alternative as follows:

$$\pi_1(F) = \min\left(\max\left(\pi_{1I}(F_R), \pi_{1I}(F_I)\right), \max\left(\pi_{2I}(F_R), \pi_{2I}(F_I)\right)\right) \quad (73)$$

since the resulting possibility degrees for friendly objects are higher than for (65). (Note that, in reality, combination (73) would not be selected for F for the same reasons as mentioned above regarding $S2$.) Using these possibility degrees for friendly objects, and applying *dec*2 decision rule for $S2$ combination ($\pi_{I\min}(M)$ for the IR, $\pi_G(M)$ for the GPR, and (63) for fusion of the two with the MD), four mines out of 21 are wrongly classified. This illustration shows to which extent a careless selection (that does not take into account the specificities and differences of the corresponding risks for this type of application) of the combination operators could be dangerous.

C. Robustness

For each of the sensors, in the modeling step, some parameters are introduced, and their values are chosen based on our knowledge. These values are being understood as examples in cases where no specific information is provided and can be adapted in the function of the additional knowledge. To test the robustness of the results, we have tuned the values of the parameters, and we have obtained the results as follows. Note that the two methods are equally robust, and that, in most of the cases, the robustness is so high that we have tested unrealistic values to have a change in the number of detected mines and/or false alarms.

In case of the IR measures, we have changed the values of a_1 and a_2. If a_1 is 15 cm^2, the IR as well as the fusion results remain unchanged for all values of a_2 higher than 60 cm^2. Below that value, the IR performance starts to decrease; however, the final fusion results remain unchanged. If a_2 is 225 cm^2, the IR and fusion results are unaffected as long as the a_1 value is lower than 140 cm^2. Above that value, the IR performance starts to decrease; however, the fusion results, again, remain unchanged. We have also performed tests in which we change the central point $0.5(a_1 + a_2)$ and keep the interval $a_2 - a_1$ fixed and vice versa, and the results are again highly robust. Similar tests are performed, and comparable robustness is experienced with the range of expected sizes of metal in mines in case of the MD.

As far as the GPR measures are concerned, for each of the parameters $D_{\max}$, m_d, p, v_t, and h, we have analyzed the influence of their value on the results. As an example of corresponding receiver operating characteristic (ROC) curves (ROC is a plot of the probability of detection versus the false alarm rate as a function of the threshold setting on the output decision variable [5]), Fig. 4 contains results obtained by varying the values of parameter $D_{\max}$. Since the number of mines and false alarms is not statistically high, absolute values (number of detected mines and of false alarms) are shown instead of rates. Note that if the $D_{\max}$ value is higher than 9 cm, the GPR and final fusion results are unchanged, so the resulting ROC curves are obtained for values of $D_{\max}$ equal to or smaller than 9 cm, and that a significant drop in the number of detected mines (lower than 9 out of the maximum 13 in case of the GPR and 19 for the fused results) occurs for $D_{\max}$ values smaller than 5 cm. For m_d values in the range [20, 865], the final fusion results remain the same as initially, whereas the GPR results start to change if that value is below 400 or above 750. In case of p, as long as it is higher than 250, the fusion results are unaffected, whereas the GPR results

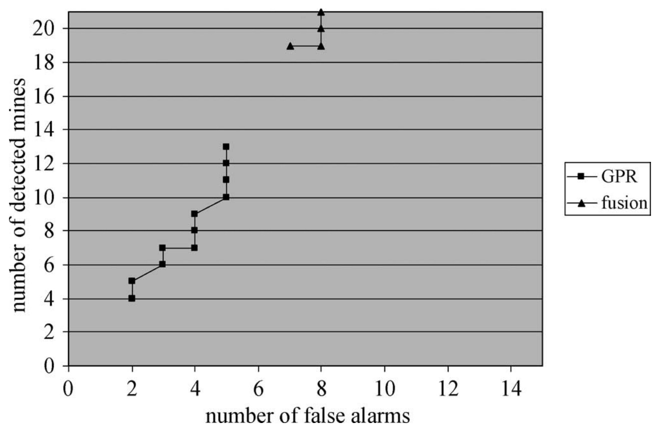

Fig. 4. ROC curve for the $D_{\max}$ parameter.

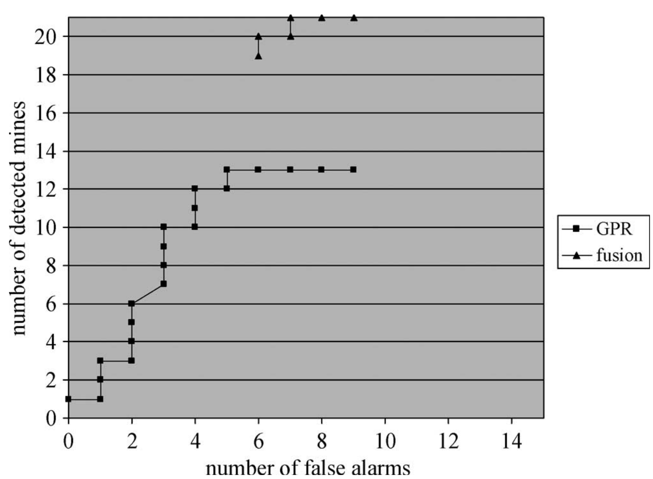

Fig. 5. ROC curve for the h parameter.

are stable if the value of this parameter is higher than 350. If v_t is in the range $[0.76 \times 10^8 \text{ m/s}, 1.64 \times 10^8 \text{ m/s}]$, the fusion results do not change; the corresponding range for the GPR is $[1.1 \times 10^8 \text{ m/s}, 1.64 \times 10^8 \text{ m/s}]$. Last, another example of corresponding ROC curves is shown in Fig. 5, obtained by varying the values of parameter h. Note that for any value of this parameter above 2.5×10^7 m/s, the fusion results remain unaltered.

None of the parameters is chosen based on the specific data set but on the general knowledge we have regarding AP mines and humanitarian mine detection, together with the literature overview we have performed. Being aware that these knowledge and experience might be incomplete, parameters are chosen so as not to introduce unavailable information, and we experience excellent robustness of the results with respect to their tuning. Thus, the values of the parameters can be understood as examples, and, for each of the parameters, the interval of the values that do not affect the final fusion result is very wide.

VI. Conclusion

A novel method for the fusion of measures extracted from heterogeneous sensor data is proposed in the framework of humanitarian mine detection. The method is based on the possibility theory. The sensors, based on radar techniques, MDs, or infrared images, provide complementary information about the nature of the observed object.

This method has been compared to a previously developed method based on belief functions. The differences at the combination step are mainly highlighted in this comparison. The modeling step is performed according to the semantics of each framework; however, the designed functions are as similar as possible to enhance the combination step. In particular, we propose different fusion operators depending on the information and its characteristics, whereas all pieces of information are combined using Dempster's rule in the belief function framework.

We have shown that appropriate modeling of the data along with their combination in a possibilistic framework leads to better decision making, i.e., better differentiation between mines and friendly objects. The decision rule is designed to detect all mines at the price of a few confusions with friendly objects. This is a requirement of this particular application domain since it is better to ask a deminer to search for an object that is finally friendly than to assure him that an object is friendly while it is a mine. Still, the number of false alarms remains limited in our results. The robustness of the choice of the operator (within a class corresponding to the type of reasoning we want to achieve) is also demonstrated since all mines are detected for all fusion schemes and for a wide range of the parameters. The obtained experimental results should be considered as a proof of concept, whereas a future work could be a complete validated application, which asks for further tests on some other real data sets and other sensors.

The proposed modeling is flexible enough to be easily adapted to the introduction of new pieces of information about the types of objects and their characteristics, as well as of new sensors.

Acknowledgment

The authors would like to thank the Netherlands Organization for Applied Scientific Research Physics and Electronics Laboratory (The Hague, The Netherlands) for the permission to work on the data gathered on their test facilities within the Dutch HOM-2000 project.

References

[1] G. Shafer, *A Mathematical Theory of Evidence*. Princeton, NJ: Princeton Univ. Press, 1976.
[2] D. Dubois and H. Prade, "Possibility theory and its applications: A retrospective and prospective view," in *Decision Theory and Multi-Agent Planning (CISM International Centre for Mechanical Sciences)*, G. Della Riccia *et al.*, Ed. New York: Springer-Verlag, 2006, pp. 89–100.
[3] M. L. Yee, "Multisensor probabilistic fusion for mine detection," in *Proc. SPIE—Conf. Detection Remediation Technologies Mines Minelike Targets*, Orlando, FL, 2001, vol. 4394, pp. 959–969.
[4] F. Cremer, K. Schutte, J. G. M. Schavemaker, and E. den Breejen, "A comparison of decision-level sensor-fusion methods for anti-personnel landmine detection," *Inf. Fusion*, vol. 3, no. 2, pp. 187–208, Sep. 2001.
[5] Y. Liao, L. W. Nolte, and L. M. Collins, "Decision fusion of ground-penetrating radar and metal detector algorithms—A robust approach," *IEEE Trans. Geosci. Remote Sens.*, vol. 45, no. 2, pp. 398–409, Feb. 2007.
[6] P. Yägerbro *et al.*, "Combination of GPR and metal detector for mine detection," in *Proc. IEE 2nd Int. Conf. Detection Abandoned Landmines*, Edinburgh, U.K., 1998, pp. 177–181.
[7] S. Auephanwiriyakul, J. M. Keller, and P. D. Gader, "Generalized Choquet fuzzy integral fusion," *Inf. Fusion*, vol. 3, no. 1, pp. 69–85, Mar. 2002.

[8] T. Aidgides, M. Fernández, and G. Dobeck, "Side scan sonar imagery fusion for sea mine detection and classification in very shallow water," in *Proc. SPIE—Conf. Detection Remediation Technologies Mines Minelike Targets*, Orlando, FL, 2001, vol. 4394, pp. 1123–1134.

[9] R. J. Stanley, P. D. Gader, and K. C. Ho, "Feature and decision level sensor fusion of electromagnetic induction and ground penetrating radar sensors for landmine detection with hand-held units," *Inf. Fusion*, vol. 3, no. 3, pp. 215–223, Sep. 2002.

[10] S. W. Perry and L. Guan, "Pulse-length-tolerant features and detectors for sector-scan sonar imagery," *IEEE J. Ocean. Eng.*, vol. 29, no. 1, pp. 138–156, Jan. 2004.

[11] N. Milisavljević and M. Acheroy, "An approach to the use of the Bayesian rule in decision level fusion for multisensor mine detection," in *Proc. PSIP*, Paris, France, 1999, pp. 261–266.

[12] P. Gader, "Signal-processing and sensor fusion methods," in *Alternatives for Landmine Detection*, J. Macdonald *et al.*, Ed. Lanham, MD: Natl Book Network, 2003, pp. 311–326.

[13] R. Voles, "Confidence in the assessment and use of mine detection systems," in *Proc. IEE 2nd Int. Conf. Detection Abandoned Landmines*, Edinburgh, U.K., 1998, pp. 28–30.

[14] S. Perrin, "Contribution à l'algorithmique multicapteur pour la détection de mines antipersonnel," Ph.D. dissertation, Ecole Centrale de Lille, USTL, Lille, France, 2001.

[15] E. den Breejen, K. Schutte, and F. Cremer, "Sensor fusion for anti personnel landmine detection," in *Proc. SPIE—Conf. Detection Remediation Technologies Mines Minelike Targets*, Orlando, FL, 1999, vol. 3710, pp. 1235–1245.

[16] B. A. Baertlein, W.-J. Liao, and D.-H. Chen, "Predicting sensor fusion performance using theoretical models," in *Proc. SPIE—Conf. Detection Remediation Technologies Mines Minelike Targets*, Orlando, FL, 2001, vol. 4394, pp. 1035–1046.

[17] N. Milisavljević and I. Bloch, "Sensor fusion in anti-personnel mine detection using a two-level belief function model," *IEEE Trans. Syst., Man, Cybern. C, Appl. Rev.*, vol. 33, no. 2, pp. 269–283, May 2003.

[18] P. Smets and R. Kennes, "The transferable belief model," *Artif. Intell.*, vol. 66, no. 2, pp. 191–234, Apr. 1994.

[19] P. Smets, "What is Dempster–Shafer's model?" *Advances in the Dempster–Shafer Theory of Evidence*, R. R. Yager, M. Fedrizzi, and J. Kacprzyk, Wiley, Eds. New York: Wiley, 1994, pp. 5–34.

[20] D. Dubois and H. Prade, "A review of fuzzy set aggregation connectives," *Inf. Sci.*, vol. 36, no. 1/2, pp. 85–121, Jul./Aug. 1985.

[21] D. Dubois, H. Prade, and R. R. Yager, "Merging fuzzy information," in *Approximate Reasoning and Information Systems*, ser. Handbook of Fuzzy Sets Series, J. C. Bezdek, D. Dubois, and H. Prade, Eds. Boston, MA: Kluwer, 1999, pp. 335–401.

[22] S. Le Hégarat-Mascle, I. Bloch, and D. Vidal-Madjar, "Application of Dempster–Shafer evidence theory to unsupervised classification in multisource remote sensing," *IEEE Trans. Geosci. Remote Sens.*, vol. 35, no. 4, pp. 1018–1031, Jul. 1997.

[23] J. Chanussot, G. Mauris, and P. Lambert, "Fuzzy fusion techniques for linear features detection in multitemporal SAR images," *IEEE Trans. Geosci. Remote Sens.*, vol. 37, no. 3, pp. 1292–1305, May 1999.

[24] J. Chanussot, J. A. Benediktsson, and M. Fauvel, "Classification of remote sensing images from urban areas using a fuzzy possibilistic model," *IEEE Geosci. Remote Sens. Lett.*, vol. 3, no. 1, pp. 40–44, Jan. 2006.

[25] M. Fauvel, J. Chanussot, and J. A. Benediktsson, "Decision fusion for the classification of urban remote sensing images," *IEEE Trans. Geosci. Remote Sens.*, vol. 44, no. 10, pp. 2828–2838, Oct. 2006.

[26] D. E. van de Vlag and A. Stein, "Incorporating uncertainty via hierarchical classification using fuzzy decision trees," *IEEE Trans. Geosci. Remote Sens.*, vol. 45, no. 1, pp. 237–245, Jan. 2007.

[27] N. E. C. Verhoest, B. De Baets, and H. Vernieuwe, "A Takagi–Sugeno fuzzy rule-based model for soil moisture retrieval from SAR under soil roughness uncertainty," *IEEE Trans. Geosci. Remote Sens.*, vol. 45, no. 5, pp. 1351–1360, May 2007.

[28] D. Dubois, M. Grabisch, H. Prade, and P. Smets, "Using the transferable belief model and a qualitative possibility theory approach on an illustrative example: The assessment of the value of a candidate," *Int. J. Intell. Syst.*, vol. 16, no. 11, pp. 1245–1272, 2001.

[29] I. Bloch and H. Maître, "Fusion of image information under imprecision," in *Series Studies in Fuzziness and Soft Computing, Aggregation and Fusion of Imperfect Information*, B. Bouchon-Meunier, Ed. Berlin, Germany: Springer-Verlag, 1997, pp. 189–213.

[30] W. de Jong, H. A. Lensen, and Y. H. L. Janssen, "Sophisticated test facility to detect landmines," in *Proc. SPIE—Conf. Detection Remediation Technologies Mines Minelike Targets*, Orlando, FL, 1999, vol. 3710, pp. 1409–1418.

[31] N. Milisavljević, I. Bloch, S. P. van den Broek, and M. Acheroy, "Improving mine recognition through processing and Dempster–Shafer fusion of ground-penetrating radar data," *Pattern Recognit.*, vol. 36, no. 5, pp. 1233–1250, May 2003.

[32] J. R. Simard, "Improved landmine detection capability (ILDC): Systematic approach to the detection of buried landmines using passive IR imaging," in *Proc. SPIE—Conf. Detection Technologies Mines Minelike Targets*, Orlando, FL, 1996, vol. 2765, pp. 489–500.

[33] N. Milisavljević *et al.*, "Comparison of belief functions and voting method for fusion of mine detection sensors," in *Proc. SPIE—Conf. Detection Technologies Mines Minelike Targets*, Orlando, FL, 2001, vol. 4394, pp. 1011–1022.

[34] P. Druyts, L. Merlat, and M. Acheroy, "Modeling considerations for imaging with a standard metal detector," in *Proc. SPIE—Conf. Detection Remediation Technologies Mines Minelike Targets*, Orlando, FL, 2000, vol. 4038, pp. 1431–1451.

[35] R. M. Haralick and L. G. Shapiro, *Computer and Robot Vision*. Boston, MA: Addison-Wesley, 1992.

[36] C. Fischer *et al.*, "Detection of antipersonnel mines by using the factorization method on multistatic ground-penetrating radar measurements," *IEEE Trans. Geosci. Remote Sens.*, vol. 45, no. 1, pp. 85–91, Jan. 2007.

[37] O. Thonnard and N. Milisavljević, "Metallic shape detection and recognition with a metal detector," in *Proc. Eur. Workshop PHOTOMEC-ETE*, Liège, Belgium, 1999, pp. 99–103.

[38] N. Milisavljević, "Analysis and fusion using belief function theory of multisensor data for close-range humanitarian mine detection," Ph.D. dissertation, Ecole Nationale Supérieure des Télécommunications, Paris, France, 2001.

[39] Y. Das, "Effects of soil electromagnetic properties on metal detectors," *IEEE Trans. Geosci. Remote Sens.*, vol. 44, no. 6, pp. 1444–1453, Jun. 2006.

[40] L. Capineri, P. Grande, and J. A. G. Temple, "Advanced image-processing technique for real-time interpretation of ground-penetrating radar images," *Int. J. Imaging Syst. Technol.*, vol. 9, no. 1, pp. 51–59, 1998.

[41] I. Bloch, "Information combination operators for data fusion: A comparative review with classification," *IEEE Trans. Syst., Man, Cybern.*, vol. 26, no. 1, pp. 52–67, Jan. 1996.

[42] N. Milisavljević, I. Bloch, and M. Acheroy, "Characterization of mine detection sensors in terms of belief functions and their fusion, first results," in *Proc. 3rd Int. Conf. FUSION*, Paris, France, 2000, vol. II, pp. ThC3.15–ThC3.22.

[43] P. Smets, "Constructing the pignistic probability function in a context of uncertainty," in *Uncertainty in Artificial Intelligence*, vol. 5, L. N. Kanal, M. Henrion, R. D. Shachter, and J. F. Lemmer, Eds. New York: Elsevier, 1990, pp. 29–39.

Nada Milisavljević received the B.E.E. degree from the University of Novi Sad, Novi Sad, Serbia, the M.Sc.E.E. degree from the University of Belgrade, Belgrade, Serbia, and the Ph.D. degree from the Ecole Nationale Supérieure des Télécommunications, Paris, France.

She is currently a Researcher with the Signal and Image Centre, Royal Military Academy, Brussels, Belgium. Her research interests include humanitarian demining, sensor modeling, information fusion, belief function theory, possibility theory, pattern recognition, and crisis management.

Isabelle Bloch (A'03–M'06) received the B.S. degree in engineering and mathematics from the Ecole des Mines de Paris, Paris, France, the Ph.D. degree from the Ecole Nationale Supérieure des Télécommunications (ENST), Paris, and the "Habilitation Diriger des recherches" from the University of Paris 5, Paris.

She is currently a Professor with the Département Traitement du Signal et des Images, ENST, Centre National de la Recherche Scientifique Unité Mixte de Recherche 5141, Laboratoire Traitement et Communication de l'Information, Paris. Her research interests include 3-D image and object processing, 3-D and fuzzy mathematical morphology, decision theory, information fusion, fuzzy set theory, belief function theory, structural pattern recognition, spatial reasoning, medical imaging, and humanitarian demining.